

Convection mapping with Swarm satellite and SuperDARN radar data

R. A. D. Fiori¹, D. H. Boteler¹, D. Knudsen², J. Burchill², C. Blais¹

¹Geomagnetic Laboratory, Natural Resources Canada, Ottawa, ON, Canada

²University of Calgary, Calgary, AB, Canada

rfiori@nrcan.gc.ca



In 2012 the European Space Agency will launch the Swarm mission to provide the best ever survey of the geomagnetic field (Fris-Christensen et al., 2006; 2008). The Swarm satellites will make continuous observations of the plasma drift, making it an ideal instrument for mapping the ionospheric convection pattern. The spherical cap harmonic analysis (SCHA) technique developed for mapping the magnetic field based on observations covering a cap-like region of the spherical Earth (Haines 1985; 1988; 2007) has been adapted for mapping convection based on ion drift measurements from the Canadian Electric Field Instrument (EFI) onboard the Swarm satellites. Previously, convection maps were generated based solely on simulated Swarm measurements. The region of the map constrained by data was limited to a narrow track surrounding the footprints of the satellite trajectory. To increase the mapping region, measurements from the SuperDARN radar array are added to the Swarm data set. It is shown that the combination of the Swarm and SuperDARN data sets increases both the region of convection constrained by measurements, and the accuracy of the resultant convection maps that could be generated based on data from either instrument alone.

Convection mapping with the Swarm satellites

The Swarm mission consists of three satellites flying in near-polar circular orbits. The lower satellite pair, Swarm A and B, will fly in a near-parallel orbit having a spatial separation of ~1° of longitude measured at the equator.

Swarm Satellite	Altitude (km)	Inclination (deg)	Period (min)
A	450	86.8	93.4
B	450	86.8	93.4
C	530	87.3	95.1

The orbit of Swarm C will drift with respect to the lower satellite pair so that by the end of the mission lifetime, the orbital planes of Swarm C and Swarm A and B will differ by 9 hours of local time.

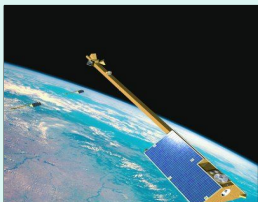


Figure 1: Illustration of the lower Swarm A and B satellite pair and the upper Swarm C satellite.

Each satellite will take ~20 minutes to cross the high-latitude region (> 50° MLAT) at a frequency of ~15 passes per day.

The B-field measured by magnetometers and the ion drift measured by the EFI can be combined to find the ionospheric E-field in the plane perpendicular to the B-field.

The Swarm satellites will make continuous observations of the ionospheric plasma drift, making it an ideal instrument for mapping the ionospheric convection flow.

Previous work has examined mapping convection based solely on Swarm data. Convection was successfully mapped based on data from 2-3 satellites, but was only constrained over a narrow region surrounding the ionospheric footprints of the satellites. The best results occurred when all 3 satellites overlapped, but such periods are infrequent. The potential for mapping ionospheric convection based on Swarm observations is better met by developing methods to constrain the convection in regions of non-overlap through the addition of velocity vectors from the SuperDARN radar network.

SCHA approach to convection mapping

SCHA has been previously developed for mapping the ionospheric convection pattern based on SuperDARN I-o-s velocity measurements (Fiori et al., 2009).

For a set of observations roughly confined to a spherical cap of angular radius (or cap-size) θ_c , the electrostatic potential is represented by series expansion

$$F_e(Q, J) = \sum_{k=0}^K \sum_{m=0}^k (g_{km} \cos mj + h_{km} \sin mj) P_{n_k(m)}^m(\cos Q)$$

- Φ_e – electrostatic potential
- θ, φ – magnetic co-latitude, longitude
- P – Associated Legendre Polynomial
- $n_k(m)$ – non-integer degree of fit
- k, m – integer degree index, order of fit
- g_{km}, h_{km} – fitting coefficients
- K – maximum degree index/order of fit

$n_k(m)$ is determined by confining the Associated Legendre Polynomial at the boundary of the spherical cap using

$$\left. \frac{dP_{n_k(m)}^m(\cos Q)}{dQ} \right|_{Q=Q_c} = 0, k - m \text{ even}$$

$$\left. P_{n_k(m)}^m(\cos Q) \right|_{Q=Q_c} = 0, k - m \text{ odd}$$

Φ_e is related to velocity by the magnetic field through

$$\vec{E} = -\nabla F_e \quad \vec{v} = \frac{\vec{E} \times \vec{B}}{B^2}$$

The fitting coefficients g_{km} and h_{km} are determined by minimizing the difference between the velocity determined by the Swarm EFI and the velocity represented above.

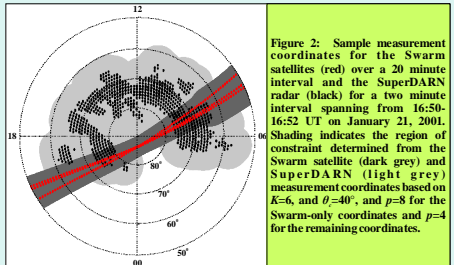
For accurate portrayal of the ionospheric plasma flow, convection should only be plotted where adequately constrained by measurements. A masking algorithm has been developed.

The minimum wavelength λ_{min} of structures that may be mapped for a given data set is given by (Haines, 1988)

$$l_{min} @ \frac{4Q_c}{K} = pDQ,$$

where $\Delta\theta$ is the angular spacing between observations, and p is the number of observations that must be present on a given wavelength. For uniformly distributed data, $p=2$. For a real data set, a $p \geq 2$ is required to ensure an accurate map. In practice, a value of $p=4-6$ is required for SuperDARN convection maps.

For each point of measurement, convection is adequately constrained within a circle radius of $\Delta\theta$, provided there are at least p data points within the circle, see Figure 2.



Simulating observations

Swarm and SuperDARN measurements were simulated based on the statistical convection for IMF B<0, B<0, and 6<B<12 with a Heppner Maynard Boundary (Ruohoniemi and Greenwald, 1996; Shepherd and Ruohoniemi, 2000), see Figure 3.

SuperDARN I-o-s velocities were generated at coordinate locations for the two-minute interval starting at 12:00 UT on January 20, 2001. Swarm measurements were determined along sample satellite A, B, and C trajectories for a 20-minute interval at a sampling resolution of 1 minute between measurements (Figure 4).

Noise was added to the data set by adding a normal distribution of $x=0$ m/s and $F=60$ m/s to the velocity magnitude and $x=0^\circ$ and $F=5^\circ$ to the velocity azimuth.

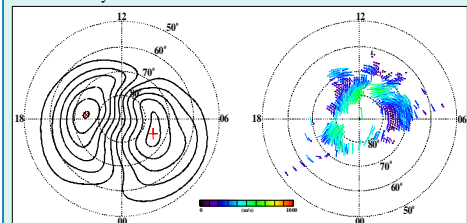


Figure 3: Statistical model convection for IMF B<0 nT, B<0 nT, and 4<B<6 with K=8. Figure 4: Simulated SuperDARN and Swarm velocity vectors.

Convection mapping with Swarm and SuperDARN data

Convection maps were generated based on Swarm measurements alone, SuperDARN measurements alone, and Swarm and SuperDARN measurements together for a spherical cap centred over the magnetic pole with $\theta_c=40^\circ$ and these variables:

Input	K	p	Figure
Swarm	2	9	4
SuperDARN	6	6	5
Swarm & SuperDARN	6	6	6

In Figure 4, 5, and 6, contours of the electrostatic potential are plotted over the region of constraint with a 6kV spacing. Velocity vectors are uniformly distributed across the region of constraint at a spacing of 2°.

Histograms indicate the difference between the north/south and east/west components of the velocity determined from the statistical model (prior to the addition of noise) and the convection velocity.

Due to the narrow track of observations, the maximum fitting order that could be supported by the Swarm-only convection maps was $K=2$, and p had to be increased to 9 to prevent unphysical characteristics in the convection map. The resultant map is significantly smoothed and the residual distribution is wide.

Addition of Swarm vectors to the SuperDARN data set did not significantly increase the region of constraint (addition of 26 points), but did improve the standard deviation of the residual value between model and output convection (reduced by half).

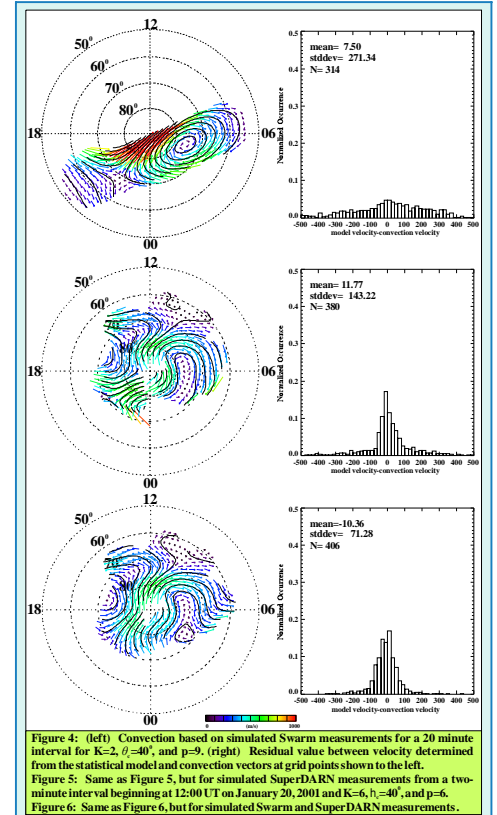


Figure 4: (left) Convection based on simulated Swarm measurements for a 20 minute interval for K=2, $\theta_c=40^\circ$, and $p=9$. (right) Residual value between velocity determined from the statistical model and convection vectors at grid points shown to the left. Figure 5: Same as Figure 5, but for simulated SuperDARN measurements from a two-minute interval beginning at 12:00 UT on January 20, 2001 and K=6, $\theta_c=40^\circ$, and $p=6$. Figure 6: Same as Figure 6, but for simulated Swarm and SuperDARN measurements.

Conclusions and future work

Simulated Swarm and SuperDARN data sets were successfully combined to generate maps of the high-latitude convection pattern, where constrained by measurements.

Addition of the Swarm vectors to a SuperDARN data set increased the accuracy of the resultant convection map over a SuperDARN-only or Swarm-only data set, despite the large number of SuperDARN vectors compared to Swarm vectors.

Additional data sets having varying degrees of SuperDARN coverage and varying locations of Swarm data sets will be tested.

Once the Swarm radar becomes operational, a validation study will be performed to ensure Swarm and SuperDARN measurements are consistent, prior to combining the data sets in practise.

References

Fiori, R. A. D., D. H. Boteler, A. V. Kossov, G. V. Haines, and J. M. Ruohoniemi (2010), Spherical cap harmonic analysis of SuperDARN observations for generating maps of ionospheric convection, *J. Geophys. Res.*, **115**, A07307, doi:10.1029/2009JA.014855.
 Fris-Christensen, E., H. Lühr, and G. Händl (2006), Swarm: A constellation to study the Earth's magnetic field, *Earth Planets Space*, **58**, 155-158.
 Fris-Christensen, E., H. Lühr, D. Knudsen, and R. Haugman (2008), Swarm-A Earth observation mission investigating space, *Advances in Space Research*, **41**, 210-216.
 Haines, G. V. (1985), Spherical cap harmonic analysis, *J. Geophys. Res.*, **90**(B3), 2583-2591.
 Haines, G. V. (1986), Computer program for spherical cap harmonic analysis of potential and general fields, *Computers and Geosciences*, **10**(4), 413-447.
 Haines, G. V. (2007), Encyclopedia of geomagnetism and paleomagnetism, chapter Spherical cap harmonic, pages 395-397, *Encyclopedia of Earth Science Series*, Springer.
 Ruohoniemi, J. M., and R. A. Greenwald (1996), Statistical patterns of high-latitude convection obtained from Goose Bay HF radar observations, *J. Geophys. Res.*, **101**(A9), 21743-21763.
 Shepherd, S. G., and J. M. Ruohoniemi (2000), Electrostatic potential patterns in the high-latitude ionosphere constrained by SuperDARN measurements, *J. Geophys. Res.*, **105**(A10), 23005-23014.